

Proc. Eurosensors XXV, September 4-7, 2011, Athens, Greece

AlN-based piezoelectric micropower generator for low ambient vibration energy harvesting

F. Stoppel^{a*}, C. Schröder^a, F. Senger^a, B. Wagner^a, W. Benecke^a

^aFraunhofer Institute for Silicon Technology ISIT, 25524 Itzehoe, Germany

Abstract

In this paper a resonant micropower generator based on the transverse piezoelectric effect is presented. The generator consists of a large silicon mass attached to an polysilicon cantilever covered with an AlN thinfilm as piezoelectric material. To maximize the power density of the generator, a parametric study by means of analytical modeling and FEM simulation has been performed. Different optimized generators with resonance frequencies in the range from 100 Hz up to 1 kHz have been designed and fabricated, using dedicated MEMS technology processes. First unpackaged prototypes showed a quality factor of about 500 under atmospheric pressure and were able to generate an electrical output power of up to 1.9 μW at an external acceleration of 1.6 m/s^2 .

© 2011 Published by Elsevier Ltd. Open access under [CC BY-NC-ND license](https://creativecommons.org/licenses/by-nc-nd/4.0/).

Keywords: piezoelectric; micropower; generator; energy; harvesting; AlN

1. Introduction

From the beginning of research within the field of micro energy harvesting a lot of work on piezoelectric generators has been done. Most of this work is focussing on PZT as piezoelectric material due to its high piezoelectric coefficients [1,2]. Since the generator performance also strongly depends on the permittivity and the Young's modulus of the piezoelectric material, AlN is a suitable alternative to PZT, offering a good compatibility to MEMS processes and overcoming the need for special poling treatments [3]. To examine maximum power densities of AlN-based and PZT-based generators a simple generator configuration consisting of a large silicon mass attached to a polysilicon cantilever covered with metal electrodes and a piezoelectric thinfilm has been investigated.

* Corresponding author. Tel: +49-4821-17-4505; Fax: +49-4821-17-4590.
E-mail address: fabian.stoppel@isit.fraunhofer.de.

2. Analytical Modeling

The dynamic behavior of the generator is described by a novel bidirectional coupled segmented analytical model, assuming a damped harmonic oscillator with an effective mass of $m_{eff} \approx m_M + \frac{33}{140} m_B$, being excited by an external acceleration a . Due to the inverse piezoelectric effect the well known equation of motion for those oscillators has to be extended by an additional coupling term, resulting in:

$$m_{eff} a = -m_{eff} \frac{d^2}{dt^2} z_M - c \frac{d}{dt} z_M - z_M K + \frac{d_{31} Y_P U}{\beta h_p} \quad (1) \quad \beta = 2 \xi_B \left(\frac{l_M}{2} - \frac{l_E}{2} + l_B \right) \left(\frac{h_p}{2} + z_n \right) Y_P \quad (2)$$

$$\xi_B = \frac{6 h_{pSi} Y_{pSi} + 6 h_p Y_P}{b_B \left(h_{pSi}^4 Y_{pSi}^2 + 4 h_p h_{pSi} \left(h_{pSi}^2 + \frac{3 h_p h_{pSi}}{2} + h_p^2 \right) Y_P Y_{pSi} + h_p^4 Y_P^2 \right)} \quad (3) \quad \xi_M = \frac{6}{b_M (h_{mSi} + h_{pSi} + h_p)^3 Y_{mSi}} \quad (4)$$

In Eq. 1 z_M denotes the deflection of the mass in its center point, c the viscous damping constant, K the effective stiffness, d_{31} the transverse piezoelectric coefficient and U the voltage. The factors β and ξ are depending on the geometry of the mass, the electrodes and the cantilever as well as the Young's modulus Y and the position of the neutral axis z_n within the cantilever, see Fig. 1 (a). For simplicity mechanical nonrelevant layers like the electrodes are neglected and the mass is assumed to be a single silicon layer.

To determine the deflection z_M and the stiffness K , the curvature of the cantilever and the mass as a function of the acting force F is calculated from the appearing moments and the position of each neutral axis. Integration and combination using adequate boundary conditions lead to:

$$K = \frac{F}{z_M} = \frac{12}{\xi_M l_M^3 + 6 \xi_B l_B l_M^2 + 12 \xi_B l_B^2 l_M + 8 \xi_B l_B^3} \quad (5)$$

By applying the fundamental equation for the direct piezoelectric effect and Kirchhoff's laws with respect to the geometry of the cantilever the generated current i_p can be derived. Transformation into the frequency domain taking into account Eq. 1 to Eq. 5 gives an expression for the generated voltage U on a load resistance R , see Fig. 1 (b), with ω and j denoting the angular frequency and the imaginary unit:

$$U = \frac{j \omega d_{31} \beta m_{eff} a b_E l_E K h_p R}{(j \omega d_{31}^2 b_E l_E K Y_P + (j \omega K - j \omega^3 m_{eff} - \omega^2 c) h_p C_p) R + (K - \omega^2 m_{eff} + j \omega c) h_p} \quad (6)$$

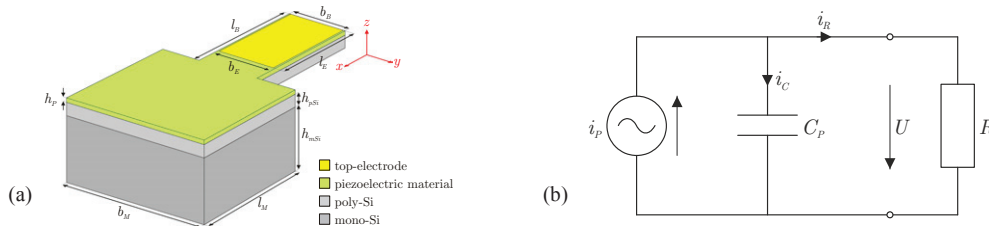


Fig. 1. (a) dimensions used for analytical modeling and FEM simulation with different lengths l , widths b and heights h ; (b) equivalent circuit model with piezoelectric current source i_p , piezoelectric capacitance C_p , load resistance R and voltage U

3. Parametric study

Using the described analytical model, a detailed parametric study has been performed, showing that AlN-based generators are able to generate the same output power as PZT-based generators, although the piezoelectric coefficient of AlN $d_{31} \approx -2.9$ pC/N is very low compared to the piezoelectric coefficient of PZT $d_{31} \approx -100$ pC/N. This is mainly due to the low dielectric constant of AlN, which is in the range of 10 to 11 and more than 100 times smaller than the dielectric constant of PZT. Additionally, AlN has a four times higher Young's modulus of about 345 GPa, leading to higher mechanical stress under deflection.

Since the Young’s modulus of the piezoelectric material also strongly influences the position of the neutral axis, the ideal AlN thickness for maximum output power is about a factor of three smaller than the corresponding PZT thickness, see Fig. 2 (a). As an effect of the bidirectional coupling the parametric study reveals that the maximum deflection decreases and the resonance frequency increases with increasing piezoelectric coefficient $|d_{31}|$, enabling the generator to convert more kinetic energy into electrical energy, see Fig. 2 (b). A further improvement can be achieved by using short cantilevers and larger masses, increasing the mechanical stress and optimizing the mass per volume.

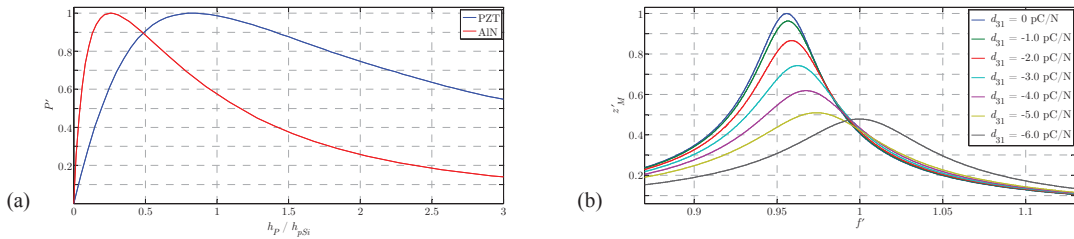


Fig. 2. (a) normalized power density P' as a function of layer thickness ratio $h_p / h_{poly-Si}$ at constant resonance frequency; (b) normalized deflection z'_M as a function of normalized frequency f and piezoelectric coefficient d_{31} at optimal load resistance

4. FEM simulation

For the investigation of more complex cantilever and electrode geometries additional FEM simulations have been done. They indicate that the output power increases and the voltage decreases as the electrode coverage of the cantilever is increased, see Fig. 3. (a). This is caused by nonuniform mechanical stress profiles and electromechanical back coupling, the latter getting worse for larger electrodes. A reduction of the back coupling can be achieved by optimizing the cantilever shape with respect to a more uniform mechanical stress profile. Due to that, trapezoidal shaped cantilevers are able to generate up to 20 % higher output power compared to rectangular shaped cantilevers, see Fig. 3. (b) and (c).

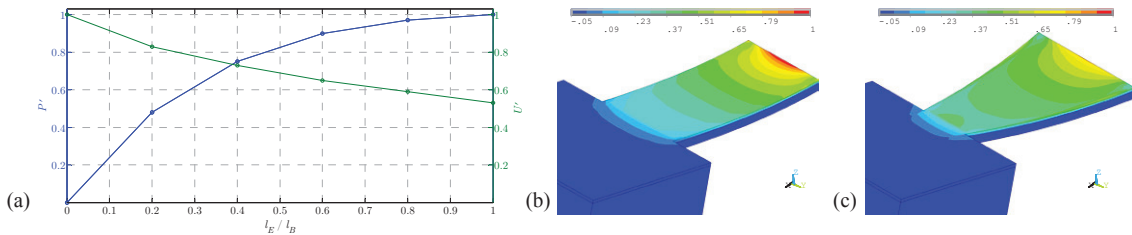


Fig. 3. (a) normalized power density P' and voltage U' as a function of electrode coverage l_E / l_B ; (b) normalized electrical potential for rectangular shaped cantilever; (c) normalized electrical potential for trapezoidal shaped cantilever

5. Design and fabrication

Based on the results of the parametric study and the FEM simulation 16 optimized generator designs including rectangular and trapezoidal shaped cantilevers, different electrode coverage and resonance frequencies of 100 Hz, 250 Hz, 500 Hz and 1 kHz have been created. For the fabrication of first AlN-based prototypes a 200 mm SOI wafer with an 11.5 μm thick polysilicon device layer is used. After depositing a 1 μm thick LPCVD SiO_2 isolation layer, a Ti/Pt bottom-electrode is evaporated and lift-off patterned, see Fig. 4 (a). This is followed by magnetron sputtering of a 2 μm thick AlN thinfilm, being structured by wet etching, see Fig. 4 (b). After realizing a sputtered Cr/Au top-electrode, see Fig. 4 (c), the cantilever and the mass are defined by DRIE and released by HF gas-phase etching, see Fig. 4 (d).

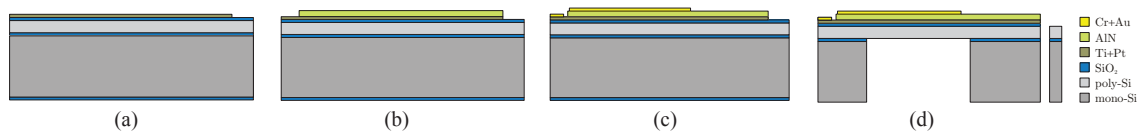


Fig. 4. process flow: (a) evaporation and lift-off of Ti/Pt bottom-electrode; (b) sputtering and wet etching of AlN piezoelectric thinfilm; (c) sputtering and wet etching of Cr/Au top-electrode; (d) DRIE and release etch of polysilicon cantilever and silicon mass

6. Characterization

First unpackaged generator prototypes with $2\ \mu\text{m}$ thick AlN and resonance frequencies of 100 Hz and 250 Hz have been characterized under atmosphere. Therefore they are assembled on PCB, mounted on an electromagnetic shaker and connected to their optimal load resistance, see Fig. 5 (a). By applying a sinusoidal excitation at varying frequency and different accelerations, the voltage generated at the load resistance is measured. Prototypes designed for 100 Hz resonance frequency generate an output power of up to $0.8\ \mu\text{W}$ at 105.6 Hz, $1\ \text{m/s}^2$ and $21\ \text{M}\Omega$, showing a slightly nonlinear frequency response due to stiffening at larger deflections, see Fig. 5 (b). Prototypes designed for 250 Hz resonance frequency generate an output power of up to $1.9\ \mu\text{W}$ at 259.8 Hz, $1.6\ \text{m/s}^2$ and $5\ \text{M}\Omega$, achieving a quality factor of about 500, see Fig. 5 (c).

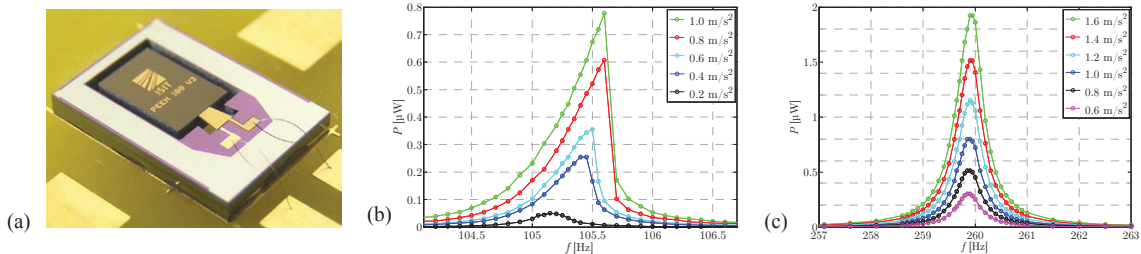


Fig. 5. (a) assembled prototype with trapezoidal shaped cantilever; measured output power P as a function of frequency f and different accelerations at optimal load resistance: (b) 100 Hz prototype @ $21\ \text{M}\Omega$; (c) 250 Hz prototype @ $5\ \text{M}\Omega$

7. Conclusion

A resonant piezoelectric micropower generator has been investigated by means of analytical modeling and FEM simulation. As the result of a detailed parametric study it could be shown that AlN is a suitable alternative to PZT as piezoelectric material, being able to generate the same output power. Different optimized generator designs with resonance frequencies in the range from 100 Hz up to 1 kHz have been fabricated, using dedicated MEMS technology processes. First unpackaged prototypes showed a quality factor of about 500 under atmospheric pressure and were able to generate an electrical output power of up to $1.9\ \mu\text{W}$ at an external acceleration of $1.6\ \text{m/s}^2$.

References

- [1] Beeby SP, Tudor MJ, White NM. Energy harvesting vibration sources for microsystems applications. *Measurement Science and Technology* 2006;17:R175–95
- [2] Anton SR, Sodano HA. A review of power harvesting using piezoelectric materials (2003–2006). *Smart Materials and Structures* 2007;16:R1–21
- [3] Elfrink R, Kamel TM, Goedbloed M, Matova S, Hohlfeld D, van Schaijk R et al. Vibration energy harvesting with aluminum nitride based piezoelectric devices. *Power MEMS* 2008;249–52